A Low Profile, Dual-band, Dual Polarized Antenna for Indoor/Outdoor Wearable Application

KASHIF NISAR PARACHA[1,2]**, (Member, IEEE),**
SHARUL KAMAL ABDUL RAHIM[1]**, (Senior Member, IEEE),**
PING JACK SOH[3]**, (Senior Member, IEEE),**
MUHAMMAD RAMLEE KAMARUDIN[4]**, (Senior Member, IEEE), KIM-GEOK TAN**[5]**,**
YEW CHIONG LO[6]**, AND MOHAMMAD TARIQUL ISLAM**[7]**, (Senior Member, IEEE)**

[1]Wireless Communication Centre, School of Electrical Engineering, Universiti Teknologi Malaysia, Skudai 81310, Malaysia
[2]Electrical Engineering Department, Government College University Faisalabad, Faisalabad 38000 , Pakistan
[3]Advanced Communication Engineering CoE, School of Computer and Communication Engineering, Universiti Malaysia Perlis, Arau 02600, Malaysia
[4]Centre for Electronic Warfare Information and Cyber, Cranfield Defence and Security, Cranfield University, Defence Academy of the United Kingdom, Shrivenham SN6 8LA, U.K.
[5]Faculty of Engineering & Technology, Multimedia University, Melaka 75450, Malaysia
[6]Faculty of Electrical Engineering, Multimedia University, Cyberjaya 63100, Malaysia
[7]Department of Electrical, Electronics and Systems Engineering, Universiti Kebangsaan Malaysia, Bangi 43600, Malaysia

Corresponding author: Kashif Nisar Paracha (paracha863@hotmail.com)

ABSTRACT A planar, low-profile, dual-band and dual-polarized antenna on a semi-flex substrate is proposed in this paper. The antenna is fabricated on Rogers substrate with a thickness of 3.04 mm and sized at $70.4 \times 76.14 \times 3.11$ mm^3 ($0.37\lambda_0 \times 0.40\lambda_0 \times 0.016\lambda_0$) only. The circular polarization property is enabled in the global navigation satellite system (GNSS) L1/E1 (lower) band by introducing a complementary split ring resonator on the antenna patch. Meanwhile, the antenna operates in the second (upper) 2.45 GHz WLAN band is enabled by etching a U-shaped slot on its ground plane. This simultaneous, dual-band and dual-polarized operation enables the proposed antenna to be applied in the indoor/outdoor wearable application. To isolate the antenna against the influence of the human body, a multiband artificial magnetic conductor (AMC) plane is added on the reverse side of the dual-band radiator. Comparison of the antenna without AMC in free space and when evaluated on the chest of a human body backed by AMC showed improved gain; from 3–5.1 dBi in the lower band, and from 1.53–5.03 dBi in the upper band. Besides that, the front-to-back ratio of the AMC backed monopole antenna also improved from 11–21.88 dB and from 2.5–24.5 dB in the GNSS and WLAN bands, respectively. Next, the specific absorption rate (SAR) of the monopole antenna with and without the AMC plane is assessed. Evaluation results indicate that the maximum SAR value decreased by up to 89.45 % in comparison with the antenna without AMC in the lower band. This indicates the effectiveness of the AMC array in increasing gain and FBR, besides reducing EM absorption in the human body.

INDEX TERMS Wearable antennas, dual-band antennas, dual-polarized antennas, circularly polarized antennas, artificial magnetic conductor (AMC) plane.

I. INTRODUCTION

One of the most challenging tasks in the future 5G network is to provide interconnection of everything, everywhere, continuously with minimal power requirements. In 2020, it is estimated that more than 50 billion devices will be interconnected, and each human is expected to be physically linked to at least ten devices. In health monitoring applications, devices are not only required to monitor the vital signs collected from the human body but also to track the user's location. For example, in the case of dementia patients, they can easily wander away from home and unable to find their way home. Such devices can either enable their family to locate them or to guide them to their destination. This can be provided if a continuous and integrated tracking and communication

system are worn by these patients to enable monitoring by their caretakers in both indoor and outdoor scenarios.

The GNSS is a space-based navigation system which provides position and time information of outdoor locations [1]. GNSS-enabled devices are used in surveying, vehicle navigation, rescue operations or tracking of military personnel, and health and activity monitoring systems. Most of these units are integrated into cellular telephones, tablet computers, cameras, and wearable outfits, watches, and even in shoes [2]. Since they are designed to be operated near the human body, there is a need to address the effects of their operation in the proximity of a human body, specifically, in the reactive near-field region in the lower frequency band.

Due to the minimal signal penetration into buildings, wearable devices equipped with GNSS capability are unable to be used indoors. Hence, it is highly desirable that a single multi-band wearable system can be used in both indoor and outdoor scenarios, and its coupling effect with the body being studied. Similarly, antennas for such devices should be integrated into a single hardware, besides being compact, conformal and operates with minimal coupling to the human body. On the other hand, for location tracking in an indoor scenario using WLAN, linearly polarized antennas are typically preferred due to its design simplicity and ability in ensuring a reliable communication link. Besides that, WLAN signals have also been proven to be able to effectively determine the location of moving users indoors [3]. It is thus imperative that all wearable systems be incorporated with such multiband, multi-polarization antennas. This is to enable linear polarization for indoor use, and operate in circular polarization for outdoor location tracking in a single hardware.

A CP characteristic for an antenna can be generated by either using a single or dual feed configuration [4]. The single feed configuration is much prevalent as it eliminates the need for power dividers typically used in dual-feed topologies. This, when combined with subwavelength resonators, have been effective in achieving multiband operation along with miniaturization of the patch antennas. Complementary Split Ring Resonator (CSRR), a popular type of resonator unit cell, has been proven to enable multiband operation [5], miniaturization [6], and CP generation onto a patch antenna proposed in [7] for a wearable glucose detection system. In that work, CP is generated by controlling the slit parameters of the CSRR to ensure a compact size at the cost of marginal realized gain of −17 dBi. The drawback of the structure is that the implantable antenna is non-planar and fed using a probe, which is unsuitable for the wearable applications.

On the other hand, the work in [8] indicated that the CSRR structure could be etched onto its feed line to introduce the required phase shift, necessary to produce two orthogonal electric fields. The generated phase difference between electric field components on the feed and ground resulted in a CP radiation characteristic for the antenna. Besides that, a compact and flexible wearable CP antenna has been introduced for 2.4 GHz WLAN communication systems, fabricated on polydimethylsiloxane (PDMS) substrate and embedded with an antenna and AMC plane made using silver nanowires (AgNWs) [9]. On the other hand, a compact low profile antenna backed by I-shaped metasurface has been proposed in [10] with LP properties for operation at 2.45 GHz.

Meanwhile, a multiband wearable antenna integrated into military beret has been proposed for indoor/outdoor positioning system [11]. The antenna operated with satisfactory performance in different worn positions on the head, at the expense of a complex feeding mechanism. Next, a dual-band and dual-polarized slotted-patch antenna embedded with modified mushroom-type structure has been proposed in [5]. The CSRR structure shifted the resonant frequency of the mushroom unit cell, whereas the diagonally-etched slot on the coaxially-fed square patch excited two mutually perpendicular modes in the 2.45 GHz band and enabled the antenna's CP characteristic. However, due to the coaxial feed and complexity of the design on the rigid substrate, implementation in wearable devices is expected to be complex. To avoid a coaxial feeding mechanism, a capacitively-coupled patch antenna has been proposed in [12]. A corner-truncated patch has been introduced to generate CP in higher 5.8 GHz band, while using capacitively coupled shorting vias pins to introduce a lower band centered at 2.45 GHz. This comes at the cost of a relatively thick structure, which is again, unsuitable for wearable applications.

This paper proposes a low profile, dual-band antenna for indoor/outdoor wearable applications. This antenna features a size reduction of about 63.86 % relative to the metamaterial-based CP slotted-patch reported in [8], and 14.87 % compared to other EM-coupled CP antenna designs [13], [14] in terms of lowest operating wavelength. The antenna uses CSRR for size reduction as well as to enable CP properties in the lower band without using any via, contrary to [7], or the dual probe feeding techniques proposed in [15]. To improve the gain and FBR of the antenna, a compact and multiband AMC unit cell has been designed. The proposed unit cell enabled up to 31.78 % of size reduction in comparison to a conventional square unit cell designed on the same substrate and inter-cell distance. Furthermore, the proposed AMC backed antenna exhibits a gain improvement of up to 3.47 dBi. Besides that, this structure also increased the antenna FBR up to 21.88 dB in the lower band and 22 dB in the upper band when assessed in the proximity of real human body, in comparison to a monopole antenna without AMC radiating in free space. The proposed AMC backed antenna also resulted in a reduced SAR by up to 89.45 % in comparison with the antenna without AMC in the lower band.

This article is presented as follows. In the next section, the design and operating principles of the proposed multiband, multi-polarization antenna are discussed. Next, section III, explains the design and integration of the metamaterial unit cell which has been designed to reduce its back radiation. Finally, its operation in the proximity of the human body in a wearable scenario is validated in Section IV, prior to the concluding remarks.
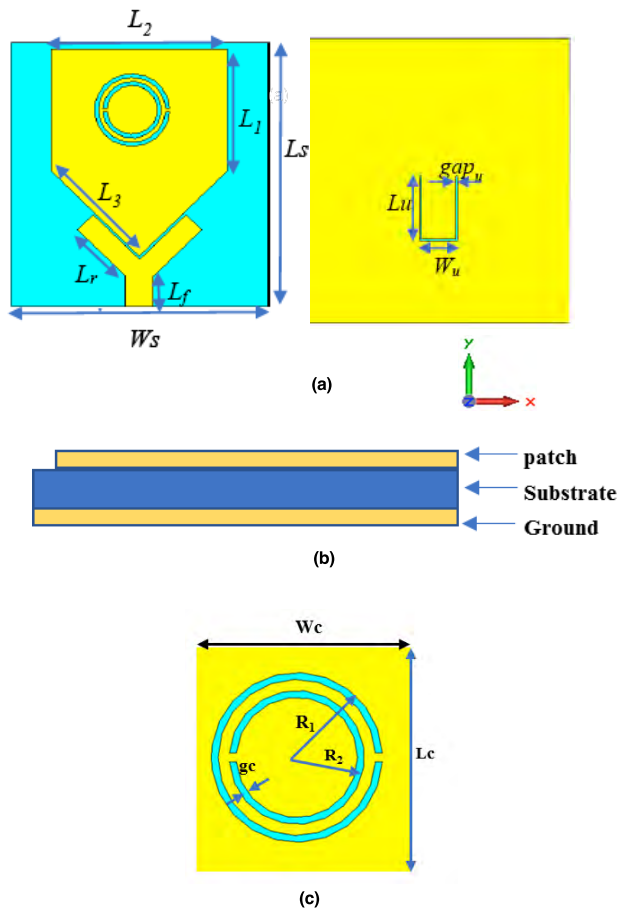
FIGURE 1. (a) Front and back view of the antenna (b) Side view of the antenna (c) CSRR unit on the patch.

FIGURE 2. Current distribution of the proposed antenna at 1.575 GHz (L1 band) for different time events ωt (a) 0^0, (b) 90^0, (c) 180^0, and (d) 270^0.

II. ANTENNA DESIGN AND ANALYSIS

A. ANTENNA DESIGN AND WORKING MECHANISM

The proposed multi-band CP/LP antenna designed on a semi-flexible substrate is shown in Figure 1. The antenna is fabricated on a Rogers substrate (RO3003C $\varepsilon_r = 3$, $\tan\delta = 0.0014$) with a thickness of 3.04 mm and sized at $70.4 \times 76.14 \times 3.11$ mm^3 ($0.37\lambda_0 \times 0.40\lambda_0 \times 0.016\lambda_0$, where $\lambda_0 = 190$ mm at $f_L = 1.575$ GHz). The design is based on a pentagonal-shaped patch etched on the substrate and fed by a Y-shaped electromagnetic (EM) coupled feed line.

In general, a CSRR has been introduced on the patch to excite two orthogonal radiation fields with 90^0 phase difference to result in CP characteristics in the lower band centered at 1.575 GHz. On the other hand, the second (upper) band is produced by introducing a U-shaped slot on the ground plane, see Figure 1(a). Adjustments of the geometric parameters of the CSRR introduces the required orthogonal phase shifts of 90^0 in two modes to result in the desired CP radiation characteristics [7]. Moreover, the choice of the CSRR is to ensure that the antenna gain and other radiation properties remain unaltered [8]. More specifically, the axial ratio (AR) in this lower band can be tuned by varying parameters such as
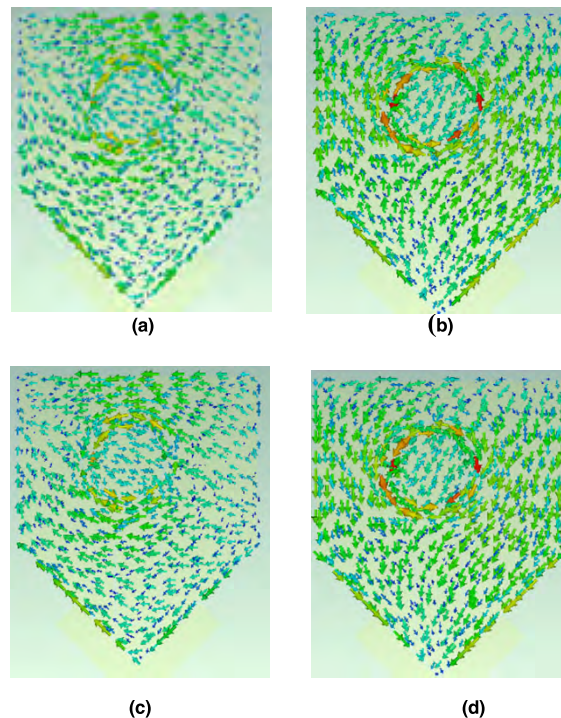
the radius of the outer ring (R_1), radius of the inner ring (R_2) and air gap (g_c) of the rings in the CSRR unit.

Besides the CP characteristics, the introduction of the CSRR structure simultaneously resulted in an additional 5% miniaturization of the antenna structure, in comparison to the pentagonal patch radiator without the CSRR. In this case, the proposed antenna sized at 74.6×70.4 mm^2($0.4 \lambda_0 \times 0.37\lambda_0 = 0.148 \lambda_0^2$, where $\lambda_0 = 190$ mm at 1.575 GHz) obtained a total of 63.86 % size reduction in comparison to the 80×80 mm^2($0.64 \lambda_0 \times 0.64\lambda_0 = 0.4096\lambda_0^2$, where $\lambda_0 = 124$ mm at 2.45GHz) antenna reported in [8] in terms of size. In [8], the defected CSRR is introduced to widen the AR bandwidth by introducing three modified CSRR at the expense of the larger size and complexity of the design.

To demonstrate the CP behavior of this antenna at the frequency of interest, the surface current distribution on the patch is simulated and depicted in **Figure 2** for $\omega t = 0^0, 90^0$, 180^0 and 270^0. It can be observed that the magnitudes of the current distribution at the 0^0 and 90^0 are equal to 180^0 and 270^0, respectively, with opposite phases. The rotation of the current distribution in an anti-clockwise fashion indicates the RHCP property of the antenna.

• *Orientation of Slits in the CSSR*

It is observed that the orientation of the slits in the CSRR affects the polarization sense of the antenna. If the rectangular slits in the CSRR are cut in the opposite direction of that in the proposed design shown in Figure 3, the antenna will then produce a LHCP characteristics instead of RHCP. Hence,
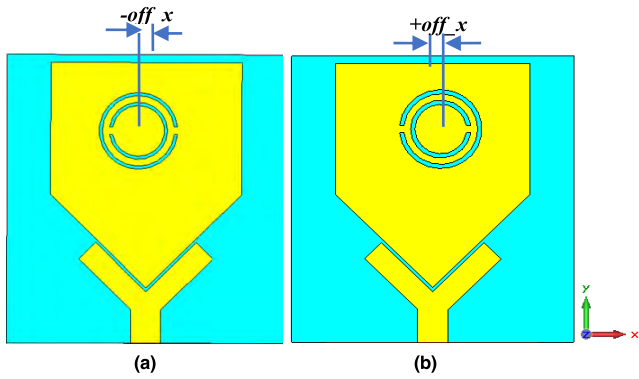
FIGURE 3. Orientation of slits for generation of (a) RHCP, (b) LHCP.

the proposed design can be easily tuned to result in RHCP and LHCP radiation properties by changing the orientation of the slits along the $\pm x$-axis. The only additional parameter that needs to be adjusted further is the horizontal displacement (*off_x*) of the CSRR with respect to the centre of the patch. Table 1 summarizes this behaviour.

TABLE 1. Controlling parameter for RHCP & LHCP generation.

Type of CP	Position of Slits	offset of CSRR along *x*-axis(*off_x*)
RHCP	0^0	-2 mm
LHCP	180^0	2 mm

B. EXPERIMENTAL EVALUATIONS OF THE CP/LP ANTENNA

Next, the optimized antenna is manufactured using the etching process generally used in printed circuit boards (PCB). The top and bottom views of the fabricated antenna are shown in **Figure 4**, with an overall size of $70.4 \times 76.14 \times 3.11$ mm^3. The reflection coefficient is measured using a Vector Network Analyzer (VNA) (model N5242A PNA-X from Agilent Technologies) and showed a good agreement with simulations. The antenna showed two distinct resonant bands from 1.564 to 1.593 GHz (1.837 %) and from 2.439 to 2.457 GHz
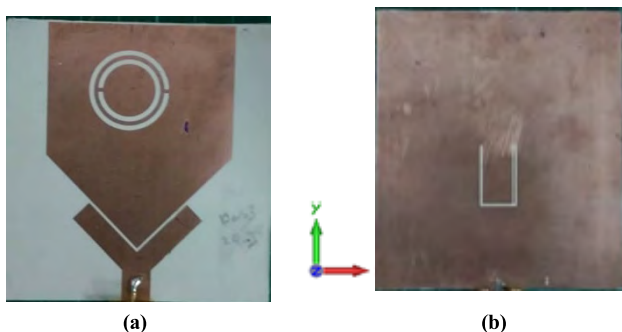

FIGURE 4. a) Top view of the fabricated prototype, (b) Bottom view.

(0.735%) for GNSS and WLAN frequencies, respectively, as illustrated in **Figure 5**.
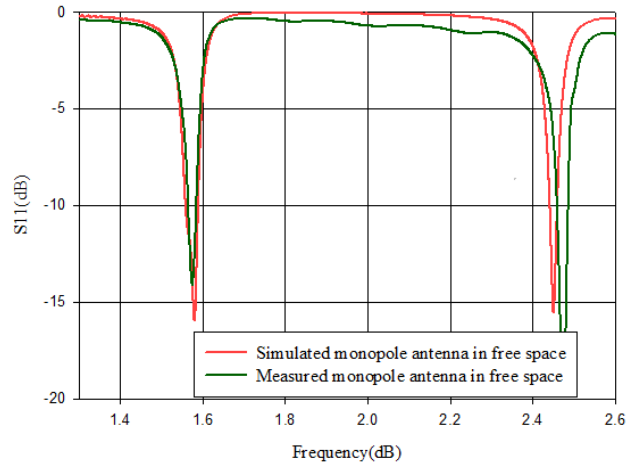

FIGURE 5. Simulated and measured reflection coefficient of the antenna working alone in the free space.

To evaluate the radiation performance of the antenna (realized gain, radiation efficiency and radiation pattern), a series of measurements was performed in an anechoic chamber. **Figure 6** depicts the AR plot of the antenna towards the boresight direction. The narrow AR bandwidth (from 1.569 to 1.581GHz) seen is due to the relatively thin (0.016 λ_0, where $\lambda_0 = 190$ mm at 1.575 GHz) substrate used. The measured radiation pattern in the two of the major axes, *yz* (E-plane) and *xz*(H-plane) planes are compared with the radiation patterns of the antenna backed by the AMC plane when placed over the voxel model and human body model in both frequency bands, as shown in **Figure 14** and **15**. The measured peak gains in the lower and upper frequency band is 3 and 1.53 dBi, respectively. The simulated radiation efficiencies are greater than 70 % throughout the two operating bands. The lower peak gain in the higher band can be attributed to the bi-directional radiation pattern of the antenna at 2.45 GHz. Meanwhile, in the lower band,
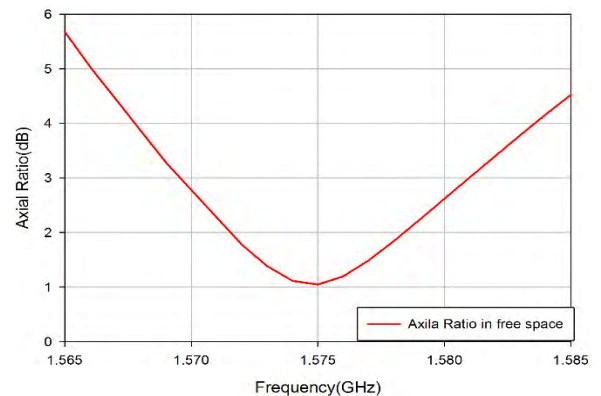

FIGURE 6. Axial Ratio plot of the antenna in boresight direction in the free space.

**FIGURE 7.** Measurement setup of the CP/LP-antenna in an anechoic chamber.

the 3dB beamwidth is 97.5^0 and 100^0 at the *xy* and *yz* planes, respectively. The FBR is calculated to be 11 dB in the GNSS band for this prototype.

Due to the bidirectional radiation in the upper band, the 3dB beamwidth is measured to be 65^0 and 79^0 at the *yz* and *xz* planes, with an FBR nearly 2.3 dB in the boresight direction. For outdoor communication, a boresight radiation characteristic is a highly desirable. Besides, the wider beamwidth in the GNSS band (approaching 120^0) is highly effective for outdoor satellite communication using wearable electronics, indicating the suitability of this antenna for the intended indoor/outdoor signal transmission. Moreover, when the antenna is evaluated on the voxel model, a maximum SAR value of 0.446 W/kg, averaged over 10g of human tissue is observed in lower band. However, since the reflection coefficient of the antenna without the AMC backing is not below -10 dB in the upper band, its SAR values are not evaluated further in this band. Care must be taken in the design process to ensure that the AMC is designed to isolate the antenna from body effects (especially in the upper band), which consequently, enhances the gain and FBR of the proposed structure for wearable application.

III. AMC BACKED CP/LP ANTENNA

To minimize coupling of the proposed antenna to the human body, especially in the second band, an AMC array is employed as the backplane of the antenna. This array is formed using a modified multiband AMC unit cell, as shown in **Figure 8**. Parallel stubs are introduced into the circular slot on the square patch. This not only introduced a dual band behavior, but also contributed to cell miniaturization of up to 31.78 % in comparison to a conventional square unit cell designed on the same substrate and inter-cell distance.

The proposed AMC backed antenna structure consists of five layers. A full ground plane occupies the bottom-most layer, followed by a thin (3.04 mm thick) RO3003C substrate. The proposed AMC will be integrated on top of this substrate, followed by a 4 mm-thick Styrofoam layer. Another 3.04 mm thick RO3003C substrate layer is then placed on top of this foam, and finally, the patch will be designed on top of this second substrate. The fabricated AMC backed antenna is shown in **Figure 9.** The choice of the semi-rigid substrate for the proposed antenna is made due to its added thermal and mechanical stability, which is limited when implemented
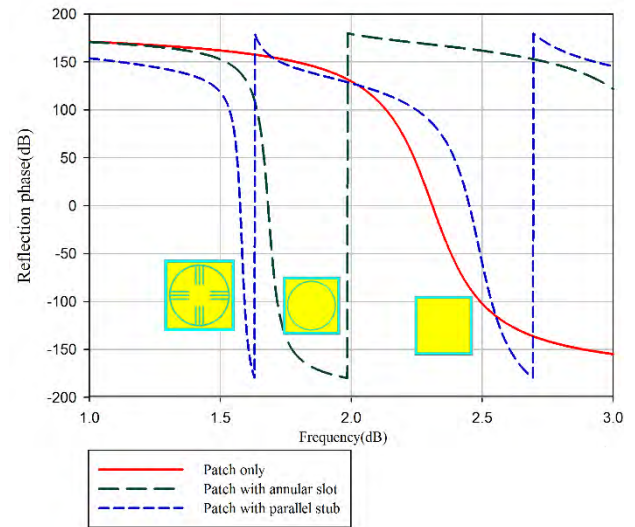
FIGURE 8. Evolution of multiband unit cell of the AMC array.

(a)   (b)
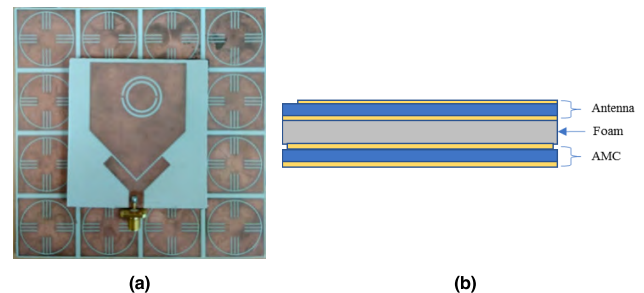
FIGURE 9. (a) Prototype of AMC backed antenna, (b) Side view of the whole structure.

on textile fabrics. Moreover, the hydrophobic behavior of the Rogers substrate makes it suitable in for operation in various environmental conditions (rain, snow, water-immersed, etc.). Due to the typically lower dielectric permitivities of textile fabrics, the resulting size of the antenna and AMC would be larger when implemented on fabrics; besides the risks of deformation such as crumpling and stretching. The overall height of the structure is 10.15 mm (0.053 $\lambda_{1.575GHz}$) which enabled a low-profile antenna structure realization [16].

A. MEASUREMENTS RESULTS AND DISCUSSIONS

The simulated and measured reflection coefficients of the CP/LP antenna with and without AMC plane in free space is illustrated in **Figure 10**. The measured operating range of the antenna with AMC is from 1.563 to 1.594 GHz (1.84 %) and from 2.434 to 2.451 GHz (0.736 %) in the GNSS and WLAN band, respectively. The AR of the antenna with AMC is much improved, with a minimum value of 0.4 dB and a wider 3 dB AR bandwidth from 1.567 to 1.580 GHz (0.83 %). In comparison, a standalone antenna without AMC only featured a 0.7 % AR bandwidth, with a higher minimum AR value of 1.4 dB. Detailed dimensions of the structure are provided in **Table 2.**
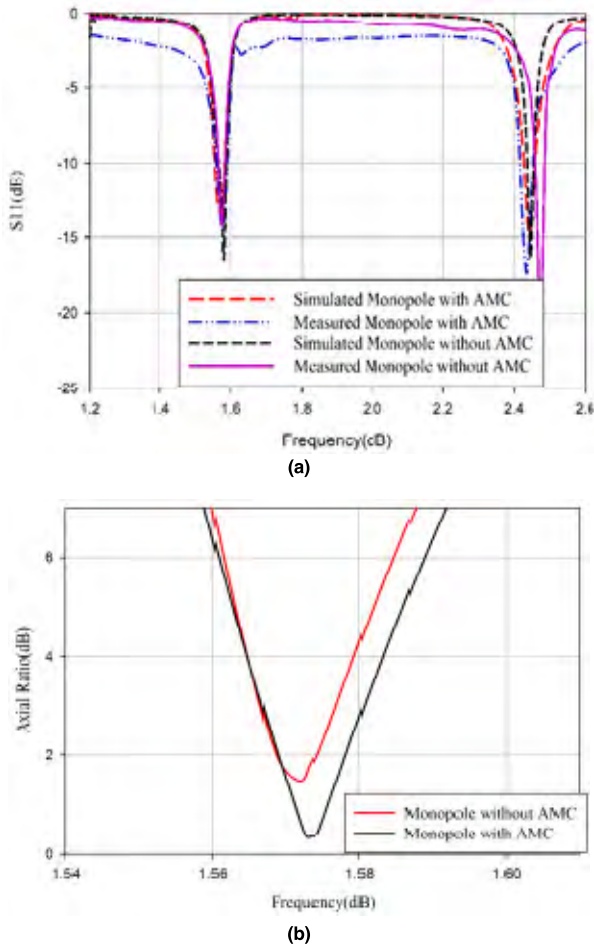
FIGURE 10. Simulated and measured results of the CP/LP antenna with and without AMC in free space: (a)S11, (b) AR.

TABLE 2. Detailed parameter of the whole structure.

Parameter	Values (mm)	Parameters	Values (mm)
L_1	24.22	L_f	8.55
L_2	24.22	L_r	18
L_3	48.4	W_s	70.4
L_s	74.6	gap_u	0.5
L_u	16.2	R_1	19.5
W_u	11.5	R_2	14.5
gc	1.1	g_f	1.05
L_c	30.5	W_c	30.5

IV. ANALYSIS OF ANTENNA

To investigate the suitability of the AMC backed antenna for wearable application, the structure is tested on a voxel model and human volunteer. The investigations in the following sections include the antenna performance and SAR.

A. EFFECTS OF HUMAN PROXIMITY (SIMULATIONS)

Ideally, wearable antennas must be designed to be insensitive to the effects of coupling to the human body. To evaluate this effect, the proposed antenna with and without AMC

are evaluated when placed over the voxel human model. A series of extensive simulations were performed, prior to their performance comparison with the same structures placed over the body of a real human volunteer. First, both structures (the standalone antenna and AMC-backed antenna) are placed at a 5 mm distance from the voxel model. Their resulting reflection coefficients indicated that the standalone antenna without the AMC backing did not perform well in the upper band (**see Figure 11**). On the contrary, its performance improved significantly in both bands when backed by the AMC plane, with the simultaneous maintenance of its polarization properties.
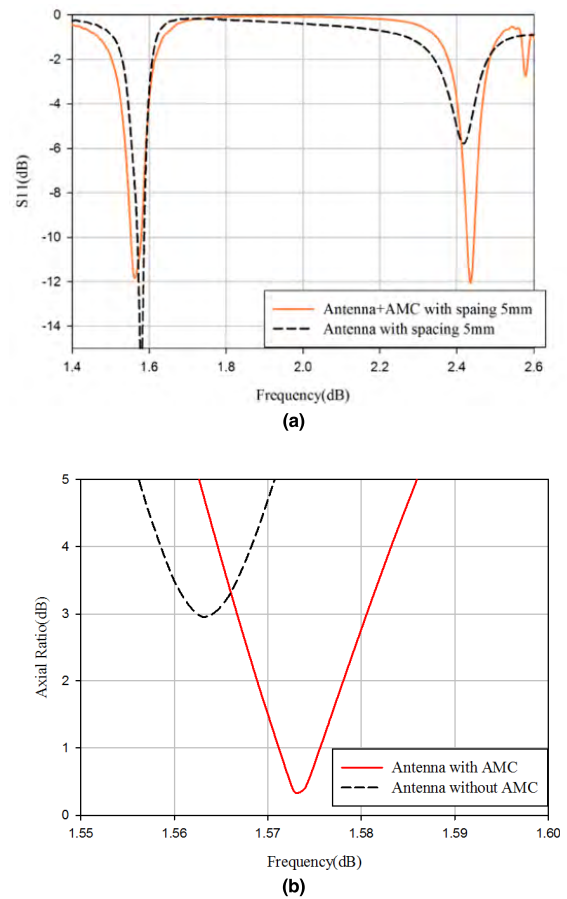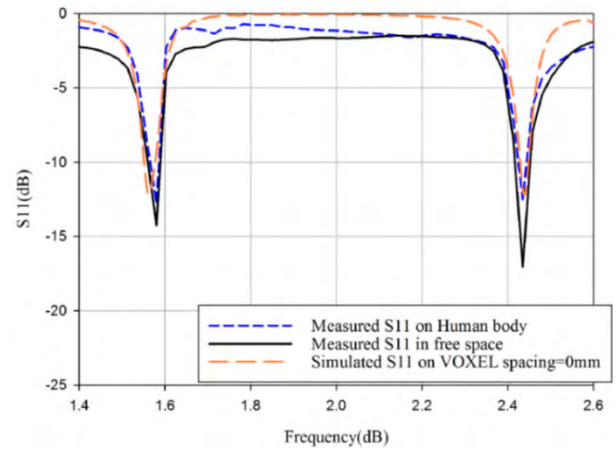

FIGURE 11. Comparison of the antenna placed over the upper torso of the voxel human model with 5mm spacing, with and without AMC in terms of; (a) reflection coefficient, (b) Axial Ratio.

To further quantify the contribution of the metasurface when placed on the body, the gap between the AMC-backed antenna and human voxel model body is varied. **Figure 12** showed that the changes in this gap do not change the reflection coefficient and AR behavior despite when being placed directly over the human model. An exception is a slight frequency shift in the minimum AR when the gap is reduced to 0 mm. This shift is due to the high dielectric loading of the body, which affected antenna polarization despite the presence of the AMC. This exhibits the insensitivity of the

(a)

(b)

FIGURE 12. Influence of the spacing between the array structure and the upper torso of the VOXEL human model on antenna's (a) reflection coefficient, (b) Axial ratio.

proposed AMC backed CP/LP antenna, making it suitable for the wearable application.

B. EFFECTS OF HUMAN PROXIMITY (EXPERIMENTAL)

Next, the antenna with AMC backing is placed at 5 mm from the chest of a volunteer human body (weight 84 kg., height 170 cm) to assess its performance in practice. **Figure 13** shows that the simulated and measured reflection coefficients of the proposed AMC-backed antenna are consistent both in free space and in the proximity of the human body. Only slight decreases in the depth of reflection coefficients are observed at the two frequencies of interest. This also indicates that the validity of the simulations performed on the voxel model in assessing wearable antennas [17].

Next, the radiation performance of the proposed antenna is then evaluated in a far-field anechoic chamber when placed on the chest of the human volunteer. The radiation pattern are measured at both the *yz*- and *xz*-planes before being compared with simulated radiation patterns obtained when the antenna

FIGURE 13. Comparison of reflection coefficients of the AMC-backed CP/LP antenna in free space, simulated on a voxel model and measured on a human volunteer.

is placed on a voxel model with 0 mm spacing. They are both illustrated in **Figures 14** and **15.** Besides that, the measured patterns of the antenna without AMC in free space are also plotted to observe the effectiveness of the AMC plane in increasing FBR and gain of the antenna. Measurements also indicated the gain of the antenna when operating on the body of a human volunteer is 5.1 dBi and 5.03 dBi at 1.575 GHz and 2.45 GHz, respectively.

On the other hand, the gain observed on the truncated voxel model is 5.4 dBi and 5.07 dBi at these same frequencies. Hence, it can be observed that the measured gain of the antenna with AMC has increased from 3 dBi to 5.1 dBi in the lower band, and from 1.53 dBi to 5.03 dBi in the upper band, in comparison to a standalone antenna in free space. There are, however, some disagreements in simulated and measured radiation patterns in the lower half plane at both major axes. This can be attributed to the following reasons: (i) the difference in the dielectric properties of the truncated voxel model in comparison to the human volunteer, and (ii) the contribution of the slight body movements which is unavoidable during measurements.

It can be observed from the radiation patterns that the FBR of the monopole antenna has increased from 11 dB to 21.88 dB (in the lower band), and from 2.5 dB to 24.5 dB (in the upper band) when backed by the AMC and assessed on the human volunteer. Hence, it can be concluded that the proposed AMC backing is effective in improving the performance of the antenna designed for the indoor/outdoor wearable application. Besides gain enhancement, the back radiation towards the human body is also reduced. Moreover, such CP/LP antenna backed by AMC designed for wearable applications are not found in literature thus far. Despite that, this work is compared with dual-band antennas backed by dual-band AMC planes in Table 4.
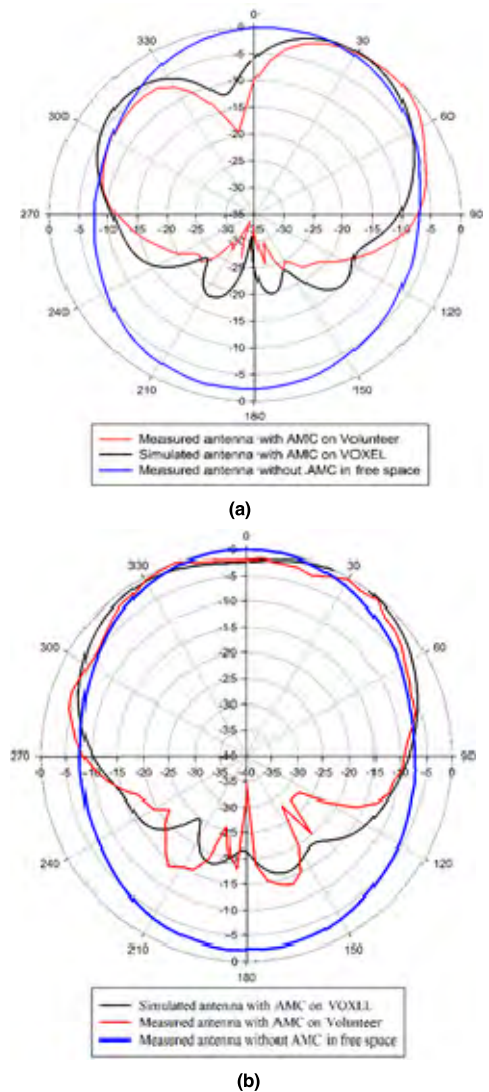
C. SPECIFIC ABSORPTION RATE ANALYSIS

As EM radiation towards the human body presents health risks, it is essential that the SAR of the AMC-backed structure
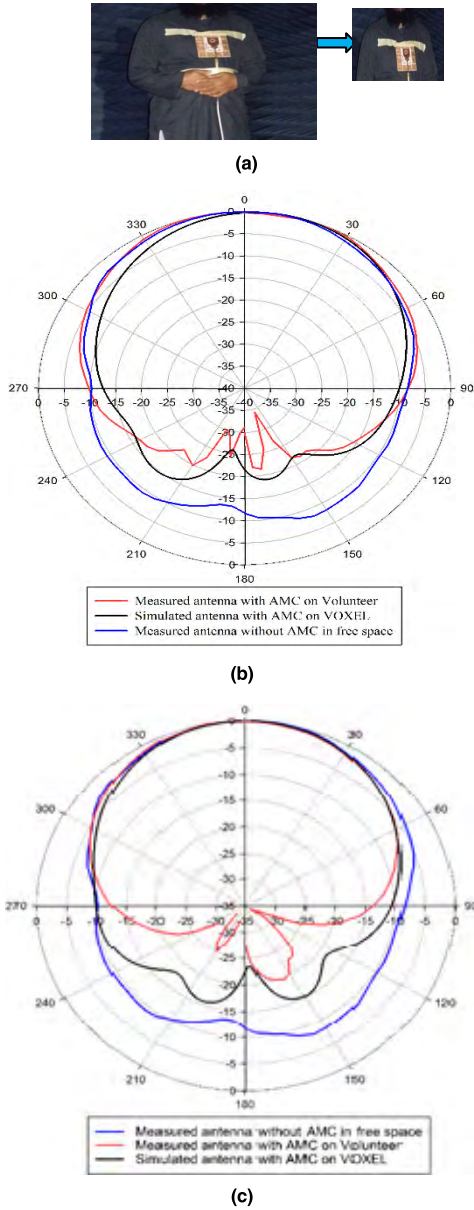
FIGURE 14. (a) Measurement setup of the AMC backed antenna on volunteer body in an anechoic chamber; and simulated and measured normalized radiation pattern plots of the structure at 1.575GHz for (b) *yz* (E-plane) axis, (c) *xz* (H-plane) axis.

FIGURE 15. Simulated and measured normalized radiation pattern plots of AMC backed antenna at 2.45 GHz for (a) *yz* (E-plane), (b) *xz* (H-plane) axis.

is evaluated. A series of simulations were performed when the antenna is placed at a 5 mm distance from different body locations, namely on the chest and arm. For this purpose, a truncated voxel model (Gustav) is used, as shown in **Figure 16(a)**. The distance of 5 mm represents the standard clothing thickness and the air gap in practice. The input power to the antenna is set to be 0.5 W (rms), and the SAR was calculated based on the IEEE/IEC 6270-1 standard, averaged over 10 g of biological tissue mass. The maximum averaged SAR values are 0.0402 and 0.0433 W/kg at 1.575 GHz and 2.45 GHz, respectively. Meanwhile, the SAR distributions calculated when the antenna is placed at 5 mm distance from

the truncated upper torso placed is illustrated in **Figure 16(b).** These values are well below the regulated limit of 2 W/kg averaged over 10 g of human tissue. Note that the maximum averaged SAR in the lower band decreased by 89.45 % compared to a standalone antenna without AMC placed at the same spacing from the voxel model. This further validated the effectiveness of the proposed AMC plane in reducing EM absorption by the human body.

To examine the characteristics of the proposed AMC plane when operated in bent conditions, the AMC-backed antenna is bent over the upper arm and forearm of a voxel human body model with radii of 45 and 30 mm. Evaluations are also performed when the antenna is bent at both the *x* and *y* axes. The resonant frequency of the antenna with AMC is well maintained below −10 dB when bent at both radii (30 mm and 45 mm) towards both axes. An exception is observed, where there is a slight change in the resonant frequency

TABLE 3. Performance of the proposed AMC backed antenna in the planar and different bending configuration over the human voxel model.

Bending radius	S₁₁(dB) x-axis	S₁₁(dB) y-axis	SAR(W/kg) x-axis	SAR(W/kg) y-axis
Flat	1.575/2.45		0.0402/0.0403	
45	1.558/2.421	1.539/2.34	0.087/0.20	0.065/0.107
30	1.568/2.435	1.549/2.26	0.125/0.26	0.08/0.165
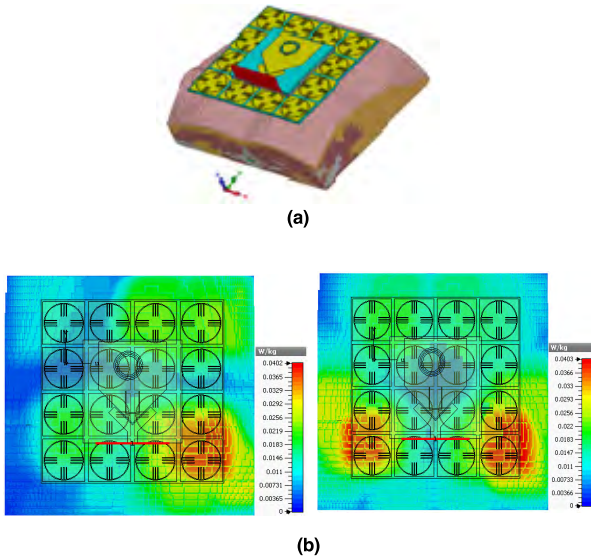
FIGURE 16. (a) AMC backed antenna over the upper torso of the VOXEL human model. (b)SAR distribution of AMC backed antenna with 5mm spacing from VOXEL (Left @1.575 GHz, Right @2.435 GHz).

the upper band, it is only 1.2 % from their respective intended frequencies.

However, when bended towards *y*-axis, the maximum shift is 2.28 % in the lower band and 7.2 % in the upper band. This is due to the strong dependence of the resonant frequency on the length of the right and left arms of the U-slot. This resulted in the more evident shift in the upper band owing to the elongation of the current path around U-slot. As expected, bending also affected the AR more severely when placed in proximity to the human body, especially when bended towards *y*-axis. However, the AR remained below 6 dB when the antenna is bent at the *x*-axis.
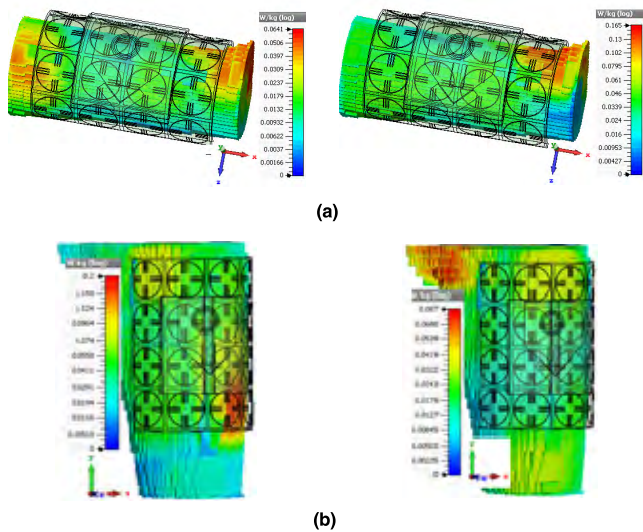
SAR distributions of the AMC-backed antenna slightly increased from 0.087 W/kg to 0.125 W/kg in the lower band as the bending radius towards *x*-axis is increased. Similarly, SAR also increased from 0.065 W/kg to 0.08 W/kg when bent along the *y*-axis. Meanwhile, SAR increased to 0.26 W/kg

in the upper band. The reflection coefficients in **Figure 17** indicated that bending has minor effects in both upper and lower bands when it is bent towards the *x*-axis. In the lower band, the maximum shift is only 1.09 %, and in the case of

TABLE 4. Comparison of the proposed AMC-backed CP/LP antenna with similar antennas available in literature.

Ref	Size	S11(% B.W.)	Material	FBR, Gain	Bands	HPBW/ARBW	AR Ratio	SAR(W/kg)
[18]	1.15ₒx1.15ₒx0.081ₒ 147x147x10 (Area=0.81ₒ²)	2.34-2.5 GHz 5.61-6.16 GHz	Fluid in PDMS	FBR 11.96/17.46 Gain 3.58/6.08	WLAN (LP/LP)	N.A	Lp/LP	SAR: <0.043 at 10mm *Pᵢₙ*=N.A.
[19]	1.1ₒx1.1ₒx0.049ₒ 135x135x`6	2.3- 2.75 GHz	Copper foil on polyester	FBR 15.6 Gain 8.5dBi	WLAN (LP)	N.A	LP only	SAR (10 mm) 0.0698W/kg *Pᵢₙ*=1W
[20]	0.9ₒx0.9ₒx0.012ₒ 150x150x2 (Area=0.81ₒ²)	1.78 to 1.98 GHz 10.92% (LP) 2.38 to 2.505 GHz 5.05%(LP)	Textile Jeans (ᵣ=1.7)	FBR 15.5/15.64 Gain 2.5/1.5	GPS/ WLAN (LP/LP)	N.A	LP only	SAR 0.024/0.016 *Pᵢₙ*=N.A.
[21]	0.89ₒx0.89ₒx0.03ₒ 60x60x2 (Area=0.79ₒ²)	4.43-4.56 GHz 4.96 – 5.01 GHz	FR4	FBR: 16.2/15 Gain: 1.87/1.56dBi	C-band (LP/LP)	N.A.	LP/LP	SAR: N.A.
[22]	0.82ₒx0.82ₒx0.024ₒ 100x100x3 (Area=0.672ₒ²)	2.45/5.8	Textile felt	FBR 15/16 Gain 2.4/4 dBi	WLAN (LP/LP)	N.A.	LP/LP	SAR:(10 mm) 0.046/0.03 Coaxial *Pᵢₙ*=0.5 W
Proposed with AMC	0.68ₒx0.68ₒx0.053ₒ 130.8x130.8x10.15 (Area=0.462ₒ²)	1.563 to 1.594 GHz (1.84 %) 2.434 to 2.451 GHz (0.736 %)	Semi-Flex	FBR 21.88/24.5 Gain 5.1/5.03 dBi	GPS/ WLAN (CP/LP)	Phi=0° 97°/121° @1.575 Phi=0° 75°/N.A. @2.45	CP/LP 1.569-1.581 (0.699%)	SAR (5 mm) 0.0402 /0.0433 *Pᵢₙ*= 0.5 W
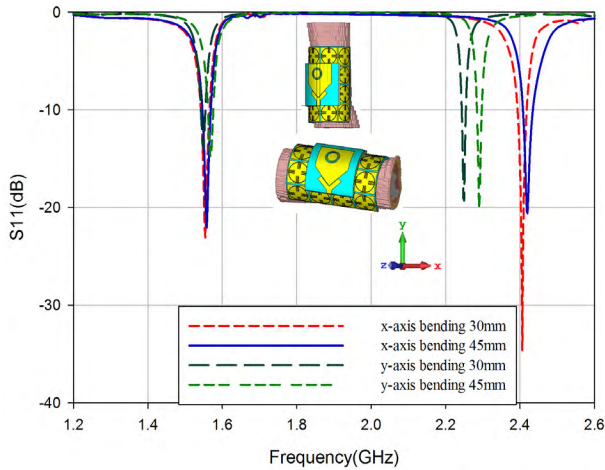
FIGURE 17. The AMC-backed antenna bent effect on the arm of a human body model with different bending radii towards x and y axis on Reflection coefficient.

(a)

(b)

FIGURE 18. SAR distribution of AMC backed antenna on the arm of Hugo model with bend radius: (a) 30mm (y-axis bending), (b) 45mm (x-axis bending).

from 0.2 W/kg in the upper band when the bending radius is increased along the *x*- axis. This small increment in SAR is also observed when the antenna is bent towards the *y*-axis, from 0.1077 W/kg to 0.165 W/kg. Nonetheless, all assessed SAR are acceptable as they do not exceed the limit of 2 W/kg averaged over 10 g of tissues. The SAR distribution on the arm when bent towards both major axes of the voxel model is shown in **Figure 18**. The performance over human voxel model is summarized in Table 3.

V. CONCLUSION

A dual-band, dual-polarized antenna designed on a semi-flexible substrate to provide for simultaneous indoor/outdoor localization and tracking using a single structure is proposed in this work. Designed based on a conventional pentagonal

patch, a CSRR is incorporated on this radiator to result in RHCP behavior in the lower GNSS (L1) band. Meanwhile, the second WLAN band is enabled by etching a U-shape slot on its ground plane. To minimize the effects of the human body on the antenna, a 4 × 4 AMC plane is designed to form the antenna's backplane. The simulated antenna performance with and without AMC are first assessed when it is placed on a voxel body model. Next, measured gain, FBR, and other radiation properties of the standalone antenna without AMC are compared with the performance of the AMC-backed antenna when worn by a human volunteer. The measured gain of the proposed structure is 5.03 dBi in the lower band and 5.07 dBi in the upper band. Meanwhile, the FBR of the AMC-backed monopole increased from 11 to 21.88 dB and from 2.5 to 24.5 dB in the GNSS and WLAN band, respectively, in comparison to a standalone antenna in free space. With the integration of the AMC plane, the maximum averaged SAR value decreased by 89.45 % relative to the standalone antenna in the lower band. This indicates that the proposed AMC structure is effective in reducing EM absorption in the human body.

REFERENCES

[1] J. J. H. Wang, "Antennas for global navigation satellite system (GNSS)," *Proc. IEEE*, vol. 100, no. 7, pp. 2349–2355, Jul. 2012.

[2] A. Dierck, H. Rogier, and F. Declercq, "An active wearable dual-band antenna for GPS and Iridium satellite phone deployed in a rescue worker garment," in *Proc. IEEE Int. Conf. RFID-Technol. Appl. (RFID-TA)*, Sep. 2013, pp. 1–5.

[3] M. Secmen and A. Hizal, "A dual-polarized wide-band patch antenna for indoor mobile communication applications," *Prog. Electromagn. Res.*, vol. 100, no. 100, pp. 189–200, 2010.

[4] W.-J. Tseng and S.-J. Chung, "A dual CP slot antenna using a modified Wilkinson power divider configuration," *IEEE Microw. Guided Wave Lett.*, vol. 8, no. 5, pp. 205–207, May 1998.

[5] K. Saurav, D. Sarkar, and K. V. Srivastava, "Dual-polarized dual-band patch antenna loaded with modified mushroom unit cell," *IEEE Antennas Wireless Propag. Lett.*, vol. 13, pp. 1357–1360, 2014.

[6] N. Nasimuddin, X. Qing, and Z. N. Chen, "A compact circularly polarized slotted patch antenna for GNSS applications," *IEEE Trans. Antennas Propag.*, vol. 62, no. 12, pp. 6506–6509, Dec. 2014.

[7] X. Y. Liu, Z. T. Wu, Y. Fan, and E. M. Tentzeris, "A miniaturized CSRR loaded wide-beamwidth circularly polarized implantable antenna for sub-cutaneous real-time glucose monitoring," *IEEE Antennas Wireless Propag. Lett.*, vol. 16, pp. 577–580, 2017.

[8] M. S. Ghaffarian, G. Moradi, and P. Mousavi, "Wide-b-and circularly polarised slot antenna by using artificial transmission line," *IET Microw., Antennas Propag.*, vol. 11, no. 5, pp. 672–679, 2017.

[9] Z. H. Jiang, Z. Cui, T. Yue, Y. Zhu, and D. H. Werner, "Compact, highly efficient, and fully flexible circularly polarized antenna enabled by silver nanowires for wireless body-area networks," *IEEE Trans. Biomed. Circuits Syst.*, vol. 11, no. 4, pp. 920–932, Aug. 2017.

[10] Z. H. Jiang, D. E. Brocker, P. E. Sieber, and D. H. Werner, "A compact, low-profile metasurface-enabled antenna for wearable medical body-area network devices," *IEEE Trans. Antennas Propag.*, vol. 62, no. 8, pp. 4021–4030, Aug. 2014.

[11] H. Lee, J. Tak, and J. Choi, "Wearable antenna integrated into military berets for indoor/outdoor positioning system," *IEEE Antennas Wireless Propag. Lett.*, vol. 16, pp. 1919–1922, 2017.

[12] X.-Q. Zhu, Y.-X. Guo, and W. Wu, "Miniaturized dual-band and dual-polarized antenna for MBAN applications," *IEEE Trans. Antennas Propag.*, vol. 64, no. 7, pp. 2805–2814, Jul. 2016.

[13] A. Torres-García, F. Marante, A. Tazón, J. Vassal'lo, J. Teniente, and M. Beruete, "Broadband circular polarized field generation in single layer microstrip patch antennas," in *Proc. 10th Eur. Conf. Antennas Propag. (Eucap)*, Apr. 2016, pp. 1–4.

[14] A. E. Torres, F. Marante, A. Tazón, and J. Vassal'lo, ''New microstrip radiator feeding by electromagnetic coupling for circular polarization,'' *AEU-Int. J. Electron. Commun.*, vol. 69, pp. 1880–1884, Dec. 2015.

[15] R. Xu, J.-Y. Li, J.-J. Yang, K. Wei, and Y.-X. Qi, ''A design of U-shaped slot antenna with broadband dual circularly polarized radiation,'' *IEEE Trans. Antennas Propag.*, vol. 65, no. 6, pp. 3217–3220, Jun. 2017.

[16] F. Yang and Y. Rahmat-Samii, ''Reflection phase characterizations of the EBG ground plane for low profile wire antenna applications,'' *IEEE Trans. Antennas Propag.*, vol. 51, no. 10, pp. 2691–2703, Oct. 2003.

[17] S. N. Makarov *et al.*, ''Virtual human models for electromagnetic studies and their applications,'' *IEEE Rev. Biomed. Eng.*, vol. 10, pp. 95–121, 2017.

[18] M. N. Ramli, P. J. Soh, M. F. Jamlos, H. Lago, N. M. Aziz, and A. A. Al-Hadi, ''Dual-band wearable fluidic antenna with metasurface embedded in a PDMS substrate,'' *Appl. Phys. A, Solids Surf.*, vol. 123, p. 149, Feb. 2017.

[19] B. S. Abirami and E. F. Sundarsingh, ''EBG-backed flexible printed Yagi–Uda antenna for on-body communication,'' *IEEE Trans. Antennas Propag.*, vol. 65, no. 7, pp. 3762–3765, Jul. 2017.

[20] S. Velan *et al.*, ''Dual-band EBG integrated monopole antenna deploying fractal geometry for wearable applications,'' *IEEE Antennas Wireless Propag. Lett.*, vol. 14, pp. 249–252, 2015.

[21] X. Zhang, Z. Teng, Z. Liu, and B. Li, ''A dual band patch antenna with a pinwheel-shaped slots EBG substrate,'' *Int. J. Antennas Propag.*, vol. 2015, pp. 1–8, 2015.

[22] S. Yan, P. J. Soh, and G. A. E. Vandenbosch, ''Low-profile dual-band textile antenna with artificial magnetic conductor plane,'' *IEEE Trans. Antennas Propag.*, vol. 62, no. 12, pp. 6487–6490, Dec. 2014.

KASHIF NISAR PARACHA received the B.S. degree (Hons.) in electrical engineering from the University of Engineering and Technology, Taxila, Pakistan, and the M.S. degree in electrical engineering from the King Fahd University of Petroleum and Mineral (KFUPM), Dahran, Saudia Arabia, in 2004 and 2008, respectively. He is currently pursuing the Ph.D. degree with the Wireless Communication Center, Electrical Engineering Department, Universiti Teknologi Malaysia, Johor Bahru, Malaysia. He has authored or co-authored about two research journal articles, and three conference articles. His research interests include communication, antenna design, metamaterials, and inkjet printing methods and algorithms. He is a member of IEEE and a life time Professional Member of the Pakistan Engineering Council.

He has been serving as a Lecturer with the EE Department, Government College University Faisalabad, since 2011. He was a Research Assistant with the EE Department, KFUPM, from 2006 to 2008, and taught in the EE Department, The University of Faisalabad, Pakistan, from 2008 to 2011. He is currently holds the Malaysian International Scholarship to pursue the Ph.D. degree at UTM.

SHARUL KAMAL ABDUL RAHIM received the degree in electrical engineering from The University of Tennessee, USA, the M.Sc. degree in engineering (communication engineering) from Universiti Teknologi Malaysia (UTM), and the Ph.D. degree in wireless communication systems from the University of Birmingham, U.K., in 2007. After his graduation from The University of Tennessee, he spent three years in industry. He joined UTM, in 2001, where he is currently a Professor with the Wireless Communication Centre. He has published over 200 learned papers, including the *IEEE Antenna and Propagation Magazine*, the IEEE Transactions on Antenna and Propagation, the IEEE Antenna and Propagation Letters, and taken various patents. His research interests include antenna design, smart antenna systems, beamforming networks, and microwave devices for fifth generation mobile communication. He is a Senior Member of the IEEE Malaysia Section, a member of the Institute of Engineer Malaysia, a Professional Engineer with BEM, a member of the Eta Kappa Nu Chapter, The University of Tennessee, and the International Electrical Engineering Honor Society. He is currently an Executive Committee of the IEM Southern Branch.

PING JACK SOH was born in Sabah, Malaysia. He received the B.Eng. and M.Eng. degrees in electrical engineering (telecommunication) from Universiti Teknologi Malaysia, in 2002 and 2006, respectively, and the Ph.D. degree in electrical engineering from KU Leuven, Belgium, in 2013.

He is currently an Associate Professor with the School of Computer and Communication Engineering (SCCE), Universiti Malaysia Perlis (UniMAP), and also a Research Affiliate with KU Leuven. From 2002 to 2004, he was a Test Engineer with Venture Corp. In 2005, he joined Motorola Solutions Malaysia as a Research and Development Engineer. There, he worked on the characterization and testing of new two-way radios' antennas and RF front-ends. In 2006, he joined SCCE, UniMAP, as a Lecturer, and also served as the Deputy Director of the Centre for Industrial Collaboration, from 2007 to 2009. He went on leave from UniMAP, in 2009, to pursue the Ph.D. degree and research attachment in KU Leuven. He was first a Research Assistant from 2009 to 2013, then a Postdoctoral Research Fellow from 2013 to 2014. He is currently a Research Affiliate with the ESAT-TELEMIC Research Division, UniMAP. His involvement in several industrial research projects such as with AGFA Healthcare Belgium resulted in a granted patent and five other filed patents. Upon his return to UniMAP, he resumed his role as a Senior Lecturer, and concurrently served as the Deputy Dean of the university's Research Management and Innovation Center, from 2014 to 2017. His research interests include wearable antennas, arrays, metasurfaces; on-body communication; electromagnetic safety and absorption; and wireless and radar techniques for healthcare applications. He is also currently an Associate Editor of the *International Journal of Numerical Modelling: Electronic Networks, Devices and Fields* (Wiley).

Dr. Soh was a recipient of the IEEE Antennas and Propagation Society Doctoral Research Award, in 2012, the IEEE Microwave Theory and Techniques Society (MTT-S) Graduate Fellowship for Medical Applications, in 2013, and the International Union of Radio Science Young Scientist Award, in 2015. He was also the Second Place Winner of the IEEE Presidents' Change the World Competition and IEEE MTT-S Video Competition, in 2013. Two of his co-authored journals were also awarded the CST University Publication Award, in 2012 and 2011. As a project advisor, his supervised students have received prizes such as the IEEE MTT-S Undergraduate Scholarship, in 2016, the First Place in the Innovate Malaysia Design Competition (Motorola Track), in 2016, and the First Place in the IEEE Malaysia Section Final Year Project Competition (Telecommunication Track), in 2015. He is a Chartered Engineer registered with the U.K. Engineering Council; a Professional Technologist registered with the Malaysia Board of Technologist; a Senior Member of the IEEE, a member of the IET, ACES, and URSI. He also serves in the IEEE MTT-S Education Committee and the IEEE MTT-S Meetings and Symposia Committee.

MUHAMMAD RAMLEE KAMARUDIN received the degree (Hons.) in electrical and telecommunication engineering from Universiti Teknologi Malaysia, Johor Bahru, Malaysia, in 2003, and the M.Sc. degree in communication engineering and the Ph.D. degree in electrical engineering from the University of Birmingham, Birmingham, U.K., in 2004 and 2007, respectively, under the supervision of Emeritus Prof. P. Hall. He was an Associate Professor with the Wireless Communication Centre, Universiti Teknologi Malaysia. He has been a Senior Lecturer with the Centre for Electronic Warfare, Information and Cyber, Cranfield Defence and Security, Cranfield University, U.K., since 2017. He holds an H-Index

of 21 (SCOPUS) and over 1700 citations (SCOPUS). He has authored a book chapter of a book *Antennas and Propagation for Body-Centric Wireless Communications* and has published over 220 technical papers in journals and proceedings, including the IEEE Transactions on Antennas and Propagation, the IEEE Antennas and Wireless Propagation Letter, the *IEEE Antenna Magazine*, the IEEE Access, the *International Journal of Antennas and Propagation*, *Progress in Electromagnetic Research*, *Microwave and Optical Technology Letters*, and *Electronics Letters*. His research interests include antenna design for 5G, MIMO antennas, array antenna for beam forming and beam steering, wireless on-body communications, in-body communications (implantable antenna), RF and microwave communication systems, and antenna diversity. He is a member of IET, an Executive Member of Antenna and Propagation, Malaysia Chapter, and a member of the IEEE Antennas and Propagation Society, the IEEE Communication Society, the IEEE Microwave Theory and Techniques Society, and the IEEE Electromagnetic Compatibility Society. He is an Associate Editor of *Electronics Letters* and *IET Microwaves, Antennas and Propagation*, and an Academic Editor for the *International Journal of Antennas and Propagation*.

KIM-GEOK TAN received the B.E., M.E., and Ph.D. degrees in electrical engineering from Universiti Teknologi Malaysia, in 1995, 1997, and 2000, respectively. He has been Senior R&D Engineer with EPCOS Singapore, in 2000. From 2001 to 2003, he joined DoCoMo Euro-Labs, Munich, Germany. He is currently an Academic Staff with Multimedia University. His research interests include radio propagation for outdoor and indoor, RFID, multi-user detection technique for multi-carrier technologies, and A-GPS.

YEW CHIONG LO received the B.Eng. degree in electronics engineering, majoring in computer, and the M.Eng.Sc. degree in microwave engineering from Multimedia University, Malaysia, in 2001 and 2005, respectively. He is currently pursuing the Ph.D. degree in microwave engineering wit Universiti Tunku Abdul Rahman, Malaysia.

From 2001 to 2005, he was a Research Officer with the Faculty of Engineering, Multimedia University, Malaysia, where he has been a Lecturer with the Faculty of Engineering, since 2005. His research interests include microwave circuits, microwave remote sensing, microwave measurement techniques, and electromagnetic compatibility.

MOHAMMAD TARIQUL ISLAM is currently a Professor with the Department of Electrical, Electronic and Systems Engineering, Universiti Kebangsaan Malaysia (UKM), and a Visiting Professor with the Kyushu Institute of Technology, Japan. He has authored or co-authored about 350 research journal articles, nearly 165 conference articles, and a few book chapters on various topics related to antennas, microwaves, and electromagnetic radiation analysis with 16 inventory patents filed. His publications have been cited 3709 times and his H-index is 33 (Source: Scopus). His Google scholar citation is 5200 and H-index is 36. His research interests include communication antenna design, radio astronomy antennas, satellite antennas, and electromagnetic radiation analysis. He was a recipient of more than 40 research grants from the Malaysian Ministry of Science, Technology and Innovation, Ministry of Education, UKM research grant, international research grants from Japan and Saudi Arabia.

Dr. Islam currently serves as the Editor-in-Chief for the *International Journal of Electronics and Informatics* and an Associate Editor for *Electronics Letter*. He was a recipient of several International Gold Medal awards, the Best Invention in Telecommunication Award, the Special Award from Vietnam for his Research and Innovation, and the Best Researcher Awards, in 2010 and 2011, at UKM. He also a recipient of the Best Innovation Award, in 2011, and the Best Research Group in ICT Niche, in 2014, by UKM. He was a recipient of the Publication Award from the Malaysian Space Agency, in 2009, 2010, 2013, and 2014, and the Best Paper Presentation Award, in 2012, the International Symposium on Antennas and Propagation, Nagoya, Japan, in 2012, and in IconSpace, in 2015. He is a Senior Member of IEEE, a Chartered Professional Engineer-CEng, Member of IET, U.K., and a member of IEICE, Japan.

● ● ●